Journal of the Serbian Chemical Society
JSCS-info@shd.org.rs • www.shd.org.rs/JSCS
J. Serb. Chem. Soc. *81* (3) 323–332 (2016)
JSCS–4849
UDC 66.017+536.5.004.12:539.4+
537.39:62–492.2
Original Scientific paper

The effects of doping on the structural, optical and electric properties of Zn_4Sb_3 material

MIRELA VAIDA[1], NARCIS DUTEANU[1]* and IOAN GROZESCU[1,2]

[1]*Politehnica University of Timisoara, Industrial Chemistry and Environmental Engineering Faculty, 6 V. Pirvan Blvd., 300223 Timisoara, Romania and* [2]*National Institute for Research and Development in Electrochemistry and Condensed Matter, 1 Plautius Andronescu Street, 300224 Timisoara, Romania*

(Received 18 September, revised 23 November, accepted 4 December 2015)

Abstract: This paper presents the results of an investigation regarding the synthesis and characterization of the thermoelectric material Zn_4Sb_3 and $(Zn_{1-x}M_x)_4Sb_3$, where M = Ag and/or Sn. The synthesis of the materials was realized by melting high purity precursors in an oven where they were kept isothermally for 12 h at 1173 K. X-Ray diffraction analysis and scanning electron microscopy were used for structural and morphologic characterization. The optical band gap for each sample was determined from absorbance spectra recorded in the visible range 240–400 nm at room temperature. The electrical resistivity as function of temperature was measured and the electrical band gap was estimated for each of the obtained samples. The semiconducting behavior of the materials was reflected in these results.

Keywords: thermoelectric; melting; electrical resistivity; band gap.

INTRODUCTION

The need for permanent discoveries in the domain of resources has influenced this area of research in the latest years. The research has attempted to find alternative sources of energy by either creating them or by regenerating and converting other types of energy. Thermoelectric materials (TE) seem to represent an alternative due to their capacity to convert wasted heat into electrical energy. The performance in the field of this type of materials is represented by the dimensionless *ZT* figure of merit,[1] which could be estimated from the equation:

$$ZT = S^2\sigma T / k \quad (1)$$

where S represents the Seebeck coefficient, σ is the electrical conductivity and k is the thermal conductivity at a certain absolute temperature T.

* Corresponding author. E-mail: narcis.duteanu@upt.ro
doi: 10.2298/JSC150918004V

An excellent TE material requires a combination of low electrical resistivity ρ ($\rho = 1/\sigma$), low thermal conductivity and a high thermopower; all of these should increase the value of *ZT*, which could lead to an increase in the range of the thermoelectric applications.[2] Considering these, devices for converting waste heat were built and these seem to be a perfect choice because they are silent, non-vibrant, with no moving mechanical parts.[3,4]

Zn_4Sb_3 is an excellent thermoelectric p-type material that presents a *ZT* of 1.3 at 650 K[1,5] and low production costs. Additionally, it is environmentally friendly compared with other expensive or toxic thermoelectric materials. It seems that its efficiency in thermoelectric conversion is due to the glass-like thermal conductivity that is offered by the disordered Zn atoms in the compound.[6,7] The material is an excellent candidate for medium temperature applications.[8]

Zn_4Sb_3 exists in four crystallographic phases: the α-phase that is stable below 263 K, the β-phase from 263 to 765 K, the γ-phase from 765 to 805 K[9,10] and the γ'-phase from 805 to 839 K.[11] Only the single β-phase has high thermoelectric properties. The Zn_4Sb_3 structure belongs to the rhombohedral space group R-3c, space group No. 167. There are 39Zn or 18Sb (1) and 12Sb (2) in each hexagonal Zn_4Sb_3 cell. Only 36 positions are available for the Zn atoms and hence, there must be at least three interstitial zinc atoms.[6]

Presently, the challenge is to improve the thermoelectric properties, and the thermal[9,12–14] and mechanical stability[12–15] of the material by using different production methods.[1,5,12,16,17] Previously reported works presented various methods that were used to obtain Zn_4Sb_3 material, *i.e.*, melt and quenching,[1,5,18–20] the melt-spinning technique,[21] the zone-melting technique,[9,12] solid state reaction,[17] thin films prepared by co-sputtering,[22] melting combined with mechanical grinding,[23,24] the gradient freeze method,[25] *etc* – good results seem to have been obtained by the zone melting method.[9] The Zn_4Sb_3 material obtained through the zone-melting technique seems to offer good thermal stability – the degradation of the material was limited.[12]

Another feature that could affect the thermoelectric properties of the material is represented by the mechanical stability. The traditional melting and quenching synthesis method often leads to a bulk Zn_4Sb_3 material that is affected by microcracks. The mechanical instability occurs due to the volumetric change at the temperature of the phase transition between the γ- and β-phases (765 K), the cause being the different thermal expansion coefficients of the γ- and β-phases.[12] It was reported that the mechanical stability of the material could be improved by reducing the average grain size of the material.[21]

Other ways to improve the thermoelectric properties of Zn_4Sb_3 is doping (addition, substitution)[26,27] with different species of ions, such as Ag,[26–29] Al,[29] Bi,[30] Cd,[31–33] Co,[34] Cu,[26] Fe,[35] Gd,[36] Hg,[37] I,[38] In,[27,39,40] Nb,[41] Pb,[27] Se,[42]

Si,[43] Sn,[19,44] Te,[20,45] *etc*. In the case of doping Zn_4Sb_3 with Ag, a significant lowering of the electrical resistivity was obtained.[28] The thermal conductivity values were remarkably reduced by doping Zn_4Sb_3 with Cu,[26] Hg,[37] Nb[41] or Te.[20]

The present paper concerns the preparation of undoped and doped Zn_4Sb_3 materials by melting the precursors at 1173 K and presents the results of the structural, morphologic, and optical analysis that were performed for the characterization of the obtained materials. Furthermore, the influence of dopants on the electrical properties of the materials was studied.

EXPERIMENTAL

Synthesis. Samples of $(Zn_{1-x}M_x)_4Sb_3$ materials were obtained using direct reaction between high purity nanopowder precursors, *i.e*., Zn (99 %), Sb (99 %), Ag (99.5 %) and Sn (99 %), where x = (0, 0.005) and M = Ag or Sn. The labeling of the samples and Ag and/or Sn doping according to formula $(Zn_{1-x}M_x)_4Sb_3$ are presented in Table I. The precursors were weighed in the stoichiometric ratio 4:3, with an excess of 2 wt. % Zn, mixed and sealed in quartz ampoules vacuumed at 7×10^{-2} Pa. The quartz ampoules were placed horizontally into an oven and heated at a rate of 303 K min^{-1} to 1173 K, where they were kept isothermally for 12 h. After cooling down to a room temperature at a rate of 303 K min^{-1}, the materials were ground in an agate mortar to obtain fine powders.

TABLE I. Undoped and Ag and/or Sn doped samples according to formula $(Zn_{1-x}M_x)_4Sb_3$

Sample	x		Chemical formula
	Ag	Sn	
S1	0	0	Zn_4Sb_3
S2	0.005	0	$Zn_{3.98}Ag_{0.02}Sb_3$
S3	0	0.005	$Zn_{3.98}Sn_{0.02}Sb_3$
S4	0.0025	0.0025	$Zn_{3.98}Ag_{0.01}Sn_{0.01}Sb_3$

Characterization techniques. Structural and morphological characterization of the obtained materials were performed using the X-ray diffraction technique (XRD) at room temperature on an X'pert Pro MPD X-ray diffractometer, with monochromatic CuK_α (λ = = 1.5418 Å) incident radiation and scanning electron microscopy (SEM, model Inspect S). The diffuse reflectance spectrum for each sample was recorded at room temperature, in the wavelength range 240–400 nm, using a Lambda 950 UV–Vis-NIR spectrometer. The obtained data were used to calculate the optical band gap (E_G) for all samples.

The electrical measurements were performed using a laboratory experimental setup. Each material sample in a glass tube of 3.8 mm diameter (d) and 10 mm length (L) was placed into an electric furnace. The two ends of the furnace were insulated using thermal insulation material and two metal electrodes were used to connect the sample with an ohmmeter. The electrical measurements were performed in the 300–500 K temperature range.

RESULTS AND DISCUSSIONS

The XRD experiments were run to establish the structure of the obtained $(Zn_{1-x}M_x)_4Sb_3$ materials and the patterns for the investigated samples are presented in Fig. 1. The patterns were recorded at room temperature in the 2θ range

of 20 to 65°. The main peaks of the recorded spectra matched the standard data of Zn_4Sb_3 (JCPDS No. 00-034-1013), but additional peaks appeared in the XRD patterns that could be ascribed to the formation of the impurity phase ZnSb (JCPDS No. 00-018-0140), which was detected in samples S1 and S2 at 2θ 23.77 and 27.89°, and for all samples at 40.05°, as indicted in Fig. 1. A peak corresponding to Zn_3Sb_2 (JCPDS 00-023-1016) was detected at $2\theta = 35.27°$ for S3.

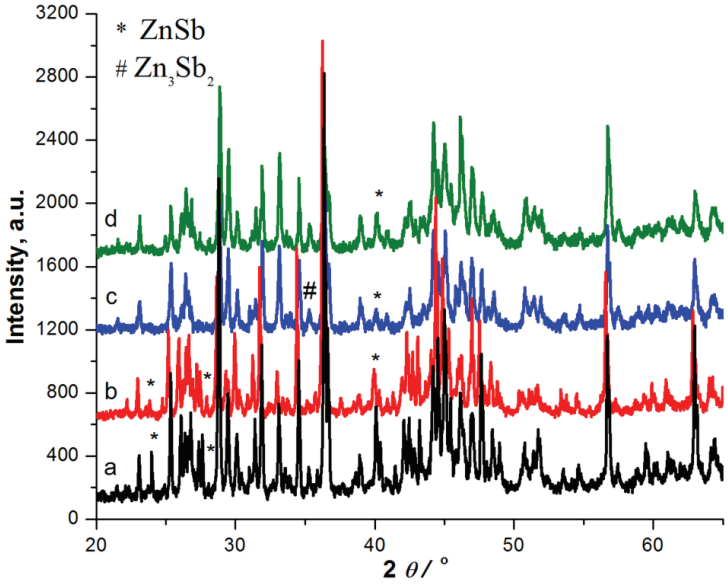

Fig. 1. X-Ray diffraction patterns for: a) Zn_4Sb_3, b) $Zn_{3.98}Ag_{0.02}Sb_3$, c) $Zn_{3.98}Sn_{0.02}Sb_3$ and d) $Zn_{3.98}Ag_{0.01}Sn_{0.01}Sb_3$.

In addition, in the XRD patterns of the doped samples, shifts in the positions of the peaks were observed. The shift was to the left for the Ag-doped sample and to the right for the Zn_4Sb_3 doped with Sn or with Ag plus Sn. The shifts of the XRD peaks are due to the change in cell parameter because the atomic radii of Ag (1.60 Å) and Sn (1.45 Å) are larger than that of Zn (1.35 Å). In the case of the sample doped with Ag, the peaks were shifted to lower 2θ values, meaning that the lattice parameters are increased. This behavior is totally opposite to that of samples S3 and S4, which can be associated to the different size of the particles of the samples.

From the SEM images, Fig. 2a–d, the surfaces morphology of the synthesized materials were revealed. The formation of agglomerates could be noticed, and polygonal and irregular-shaped particles occurred on the structures.

The absorbance spectra were obtained for all samples by converting the data from the recorded diffuse reflectance spectra, Fig. 3. Intense maximum peaks were observed for the four (S1–S4) samples at 283, 284, 285 and 282 nm, respect-

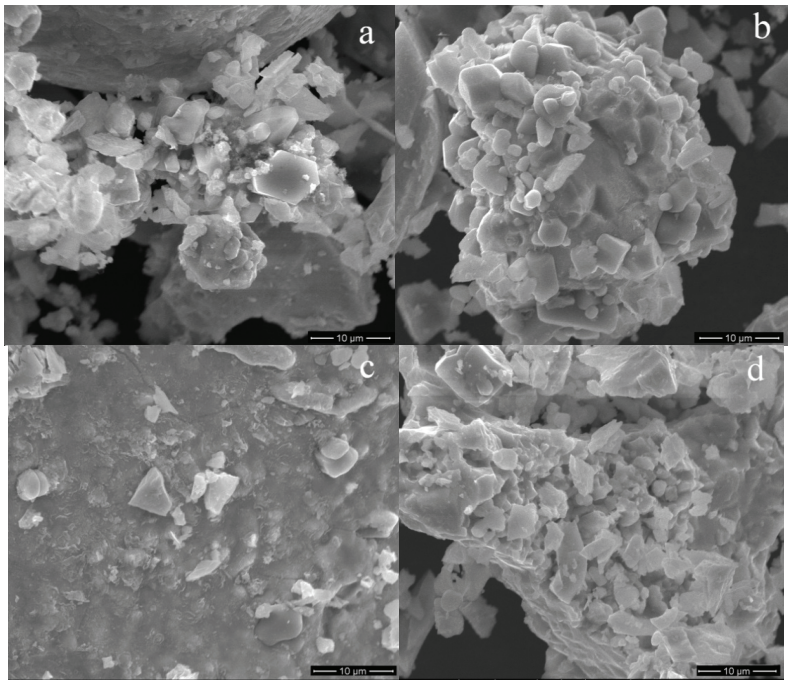

Fig. 2. The SEM micrographs for the analyzed samples of: (a) Zn_4Sb_3, (b) $Zn_{3.98}Ag_{0.02}Sb_3$, (c) $Zn_{3.98}Sn_{0.02}Sb_3$ and (d) $Zn_{3.98}Ag_{0.01}Sn_{0.01}Sb_3$.

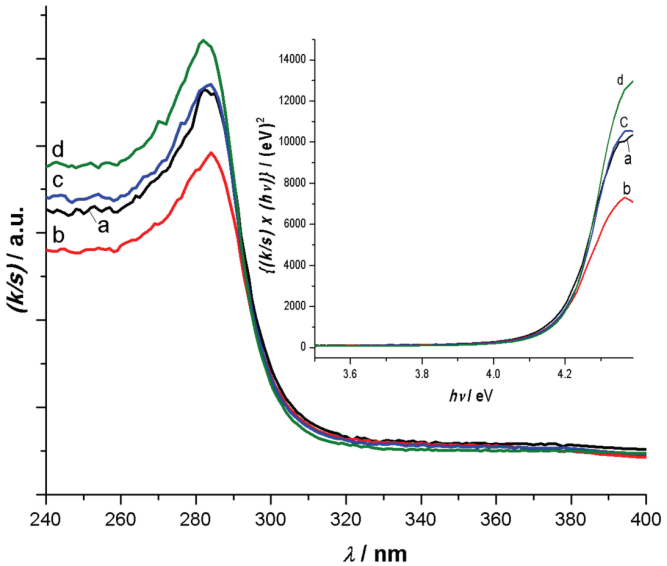

Fig. 3. The absorbance spectra for the obtained samples; a) Zn_4Sb_3, b) $Zn_{3.98}Ag_{0.02}Sb_3$, c) $Zn_{3.98}Sn_{0.02}Sb_3$ and d) $Zn_{3.98}Ag_{0.01}Sn_{0.01}Sb_3$. The optical band gaps were obtained from the inset plot.

ively. A small shift between the maximum absorption peaks was registered. In the case of the single-doped samples, the shifts of the maximum absorption peak were to higher values of λ than in the case of the undoped sample, while in the case of the double-doped sample, the maximum absorption peak appeared at a lower value of λ than in the case of the undoped sample. The obtained values for the absorbance spectra were inserted into the Kubelka–Munk equations[46,47] and then $\{(k/s)h\nu\}^2$ *vs.* $h\nu$ were plotted for each sample (inset in Fig. 3), from which the optical band gap for each sample was estimated. k denotes the absorption coefficient, s is the scattering coefficient and $h\upsilon$ represents the photon energy.

The estimated optical band gaps from Fig. 3 for the samples were E_G(S1) = = 4.00 eV, E_G(S2) = 3.98 eV, E_G(S3) = 4.03 eV and E_G(S4) = 4.06 eV.

It was observed that on doping Zn_4Sb_3 with Ag, the value for the E_G slowly decreased slightly, while for samples doped with Sn or with Ag and Sn, the optical band gap value increased. It seems like in the case of the sample $Zn_{3.98}Ag_{0.01}Sn_{0.01}Sb_3$, the lower amounts of Ag and Sn were responsible for the increase in the optical band gap to the maximum value in this set of samples.

To characterize the samples from electrical point of view, the electrical resistance (R) as a function temperature was measured for each sample. Using the geometry of the samples, the electrical resistivity (ρ) was determined for each sample using the following equation:

$$\rho = RA / L \tag{2}$$

where A represents the cross-section of the sample.

The electrical resistivity dependences on temperature in the range of 300 to 500 K for each sample of the four materials are presented in Fig. 4. It is clear that the electrical resistivity decreased with increasing temperature. The $Zn_{3.98}Sn_{0.02}Sb_3$ sample exhibited the highest electrical resistivity at room temperature, which decreased rapidly with increasing temperature, and the lowest value was observed for the double-doped sample. Ag doping ($Zn_{3.98}Ag_{0.02}Sb_3$) lowered the electrical resistivity, as was observed in previous studies.[26,27,35] The lowering of the electrical resistivity was because of an increase in the concentration of holes on incorporation of Ag into the Zn_4Sb_3 structure. Moreover, some kind of thermal hysteresis could be observed at approximately 463 K, which suggests a possible structural phase transition.

For each sample, ln ρ was plotted as a function of temperature, Fig. 5, and from this, using the linear fitting (Fig. 5, insets) for the temperature range between 385 and 415 K, the electrical band gap for each sample was estimated. The estimated electrical band gap values for the four samples were E_g(S1) = 0.85 eV, E_g(S2) = 0.96 eV, E_g(S3) = 0.94 eV and E_g(S4) = 0.90 eV. It can be seen that single doping of Zn_4Sb_3 increased the value of the electrical band gap with respect to the undoped material, while the double doping increased the electrical band gap the least.

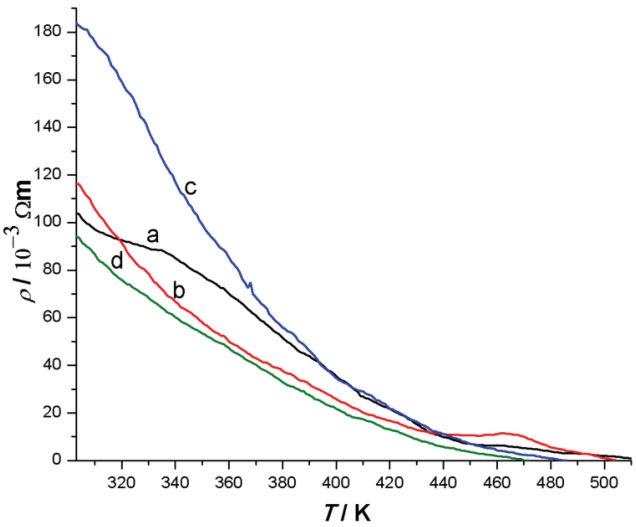

Fig. 4. The electrical resistivity dependence on temperature for: a) Zn_4Sb_3, b) $Zn_{3.98}Ag_{0.02}Sb_3$, c) $Zn_{3.98}Sn_{0.02}Sb_3$ and d) $Zn_{3.98}Ag_{0.01}Sn_{0.01}Sb_3$.

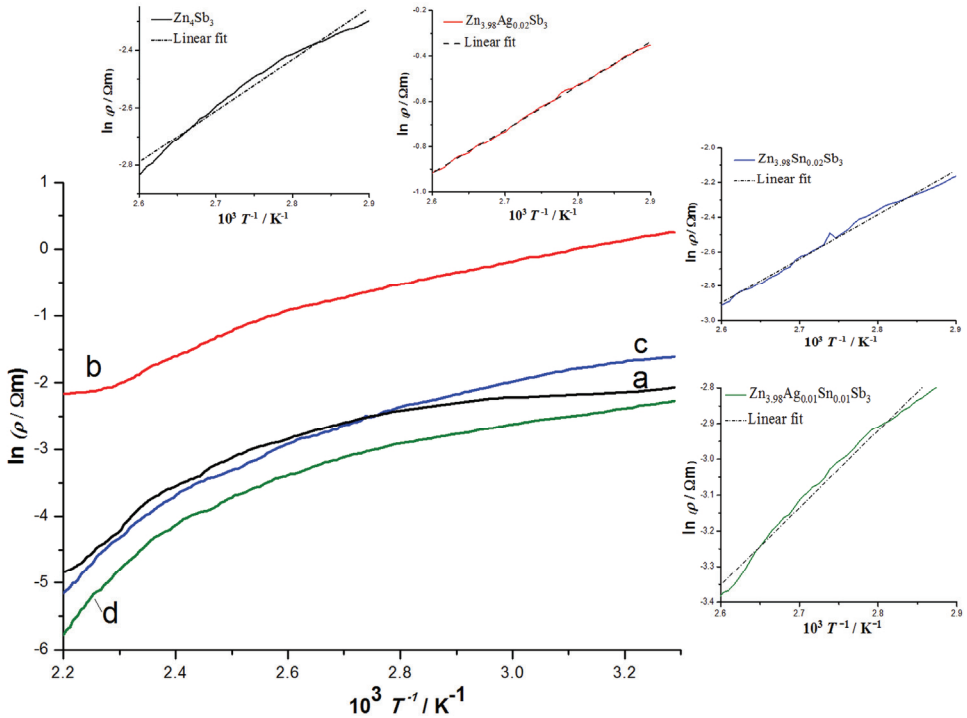

Fig. 5. From the linear fitting of ln $\rho(T)$, the electrical band gap (E_g) values were estimated for (a) Zn_4Sb_3, (b) $Zn_{3.98}Ag_{0.02}Sb_3$, (c) $Zn_{3.98}Sn_{0.02}Sb_3$ and (d) $Zn_{3.98}Ag_{0.01}Sn_{0.01}Sb_3$. The insets present the linear fit for each sample in the temperature range 385 to 415 K.

Reduction of the electrical resistivity should be favorable for higher thermoelectric performance of the materials. From the plot, it can be observed that the doping ions introduce atomic disorder in the material lattice and because of that, the doping influenced the electrical resistivity.

CONCLUSIONS

In this paper, the results of investigations regarding the influence of doping Zn_4Sb_3 with Ag and Sn ions on the structural, optical and electrical properties of the obtained materials are presented. The $(Zn_{1-x}M_x)_4Sb_3$ materials were obtained by direct reaction of the used precursors at 1173 K for 12 h. XRD and SEM measurements revealed the structure and the morphology of the obtained materials. From UV–Vis measurements, the optical band gaps for all samples were determined, which indicated that the optical band gap for the Ag-doped material was smaller than that of Zn_4Sb_3, while for the samples single-doped with Sn or double-doped with Ag and Sn, the optical band gap values were higher. Electrical measurements were performed in order to determine the electrical resistivity of the materials. The decrease in the electrical resistivity with temperature revealed the semiconducting behavior of the analyzed samples. The electrical resistivity of the material double-doped with Ag and Sn ions decreased faster with temperature than for the other samples. Electrical band gaps were determined for the obtained materials. The influence of double doping led to a lower band gap in comparison with the values for the single-doped materials.

Acknowledgements. This work was partially supported by the strategic grant POSDRU/ /159/1.5/S/137070 (2014) of the Ministry of National Education, Romania, co-financed by the European Social Fund – Investing in People, within the Sectoral Operational Programme Human Resources Development 2007–2013. The authors would like to thank the X-ray diffraction, electron microscopy and UV–Vis laboratories from the Characterization Department of the National Institute for Research and Development in Electrochemistry and Condensed Matter (Timisoara, Romania). In addition, the authors wish to thanks Malaescu Iosif (West University of Timisoara, Romania) for technical assistance during the electrical measurements.

ИЗВОД

УТИЦАЈ ДОПИРАЊА НА СТРУКТУРНА, ОПТИЧКА И ЕЛЕКТРИЧНА СВОЈСТВА Zn_4Sb_3 ПРАХОВА

MIRELA VAIDA[1], NARCIS DUTEANU[1] и IOAN GROZESCU[1,2]

[1]*Politehnica University of Timisoara, Industrial Chemistry and Environmental Engineering Faculty, 6 V. Pirvan Blvd., 300223 Timisoara, Romania u* [2]*National Institute for Research and Development in Electrochemistry and Condensed Matter, 1 PlautiusAndronescu Street, 300224 Timisoara, Romania*

У овом раду су приказани резултати проучавања процеса добијања и карактеризације термоелектричних материјала, Zn_4Sb_3 и $(Zn_{1-x}M_x)_4Sb_3$, где је M = Ag и/или Sn. Прахови су добијени топљењем веома чистих прекурсора на 1173 K током 12 h, уз накнадно млевење. Рендгенска дифракциона анализа и скенирајућа електронска микроскопија су коришћене за структурну и морфолошку анализу. Вредности оптичке енергије забрањене зоне су одређене на основу апсорпционих спектара одређених у области

таласних дужина 240–400 nm на собној температури. Одређене су и зависности електричне отпорности од температуре и прорачунате вредности електричне енергије забрањене зоне. Допирање Zn_4Sb_3 сребром доводи до смањења, а допирање калајем, или кодопирање са Ag и Sn, до смањења оптичке енергије забрањене зоне. Смањење електричне отпорности са температуром потврдило је полупроводничка својства синтетисаних узорака.

(Примљено 18. септембра, ревидирано 23. новембра, прихваћено 4. децембра 2105)

REFERENCES

1. T. Caillat, J. P. Fleurial, A. Borshchevsky, *J. Phys. Chem. Solids* **58** (1997) 1119
2. F. J. DiSalvo, *Science* **285** (1999) 703
3. S. Budak, S. Guner, R. A. Minamisawa, C. I. Muntele, D. Ila, *Appl. Surf. Sci*. **310** (2014) 226
4. W. H. Chao, S. C. Tseng, P. H. Yang, H. S. Chu, J. D. Hwang, R. J. Wu, *Surf. Coat. Technol.* **231** (2013) 34
5. E. S. Toberer, P. Rauwel, S. Gariel, J. Taftø, J. G. Snyder, *J. Mater. Chem*. **20** (2010) 9877
6. G. J. Snyder, M. Christensen, E. Nishibori, T. Caillat. B. B. Iversen, *Nat. Mater.* **3** (2004) 458
7. G. J. Snyder, E. S. Toberer, *Nat. Mater.* **7** (2008) 105
8. A V. Shevelkov, *Russian Chem. Rev*. **77** (2008) 1
9. B. L. Pedersen, B. B. Iversen, *Appl. Phys. Lett*. **92** (2008) 161907
10. H. W. Mayer, I. Mikhail, K. Schubert, *J. Less Common Met*. **59** (1978) 43
11. V. Izard, M. C. Record, J. C. Tedenac, S. G. Fries, *CALPHAD* **25** (2002) 567
12. C. Stiewe, T. Dasgupta, L. Bottcher, B. Pedersen, E. Muller, B. Iversen, *J. Electronic Mater*. **39** (2010) 1975
13. H. Yin, M. Christensen, B. L. Pedersen, E. Nishibori, S. Aoyagi, B. B. Iversen, *J. Electronic Mater.* **39** (2010) 1957
14. Y. Mozharivskyj, A. O. Pecharsky, S. Bud'ko, G. J. Miller, *Chem. Mater*. **16** (2004) 1580
15. T. Dasgupta, C. Stiewe, A. Sesselmann, H. Yin, B. B. Iversen, E. Mueller, *J. Appl. Phys*. **113** (2013) 103708
16. K. Ueno, A. Yamamoto, T. Noguchi, T. Inoue, S. Sodeoka, H. Obara, *J. Alloys Compd*. **392** (2005) 295
17. D. Cadavid, J. E. Rodriguez, *Physica, B* **403** (2008) 3976
18. D. Tang, W. Zhao, S. Cheng, P. Wei, J. Yu, Q. Zhang, *J. Solid State Chem*. **193** (2012) 89
19. X. Shai, S. Deng, D. Meng, L. Shen, D. Li, *Physica, B* **452** (2014) 148
20. D. Li, X. Y. Qin, *Intermetallics* **19** (2011) 1651
21. D. Qi, X. Tang, H. Li, Y. Yan, Q. Zhang, *J. Electronic Mater.* **39** (2010) 1159
22. Z. H. Zheng, P. Fan, P. J. Liu, J. T Luo, G. X. Liang, D. P. Zhang, *J. Alloys Compd*. **594** (2014) 122
23. C. Okamura, T. Ueda, K. Hasezaki, *Mater. Trans.* **51** (2010) 152
24. Ø. Prytz, A. E. Gunnæs, O. B. Karlsen, T. H. Breivik, E. S. Toberer, G. J. Snyder, J. Taftø, *Phil. Mag. Lett*. **89** (2009) 362
25. D. T. K. Anh, T. Tanaka, G. Nakamoto, M. Kurisu, *J. Alloys Compd*. **421** (2006) 232
26. M. Liu, X. Qin, C. Liu, L. Pan, H. Xin, *Phys. Rev., B* **81** (2010) 245215
27. F. S. Liu, L. C. Pan, W. Q. Ao, L. P. He, X. X. Li, H. T. Li, J. Q. Li, *J. Electronic Mater*. **41** (2012) 2118
28. L. Pan, X. Y. Qin, M. Liu, F. Liu, *J. Alloy. Compd*. **489** (2010) 228
29. R. Carlini, D. Marré, I. Pallecchi, R. Ricciardi, G. Zanicchi, *Intermetallics* **45** (2014) 60

30. X. Y. Qin, M. Liu, L. Pan, H. X. Xin, J. H. Sun, Q. Q. Wang, *J. Appl. Phys.* **109** (2011) 033714
31. S. Wang, H. Li, D. Qi, W. Xie, X. Tang, *Acta Mater.* **59** (2011) 4805
32. T. Caillat, A. Borshchevsky, J.-P. Fleurial, in *Proceedings of the MRS Spring Meeting,* San Francisco, March 1997, Symposium Q – Thermoelectrics, San Francisco, CA, 1997, p. 1
33. T. Souma, M. Ohtaki, *J. Alloy. Compd*. **413** (2006) 289
34. K. W. Jang, I. H. Kim, J. I. Lee, G. S. Choi, *Mater. Sci. Forum* **510**–**511** (2006) 1110
35. L. Pan, X. Y. Qin, H. X. Xin, D. Li, J. H. Sun, J. Zhang, C. J. Song, R. R. Sun, *Intermetallics* **18** (2010) 1106
36. B. Ren, M. Liu, X. Li, X. Qin, D. Li, T. Zou, G. Sun, Y. Li, H. Xin, J. Zhang, *J. Mater. Chem*., *A* **3** (2015) 11768
37. B. L. Pedersen, H. Birkedal, E. Nishibori, A. Bentien, M. Sakata, M. Nygren, P. T. Frederiksen, B. B. Iversen, *Chem. Mater*. **19** (2007) 6304
38. L. Pan, X. Y. Qin, M. Liu, *Solid State Commun*. **150** (2010) 346
39. H.-J. Gau, J.-L. Yu, C.-C. Wu, Y.- K. Kuo, C.-H. Ho, *J. Alloy. Compd*. **480** (2009) 73
40. D. Tang, W. Zhao, J. Yu, P. Wei, H. Zhou, W. Zhu, Q. Zhang, *J. Alloy. Compd.* **601** (2014) 50
41. D. Li, H. H. Hng, J. Ma, X. Y. Qin, *J. Mater. Res.* **24** (2009) 430
42. L. Pan, X. Y. Qin, M. Liu, *Solid State Sci*. **12** (2010) 257
43. L. Pan, X. Y. Qin, H. X. Xin, C. J. Song, Q. Q. Wang, J. H. Sun, R. R. Sun, *Solid State Sci.* **12** (2010) 1511
44. T. Koyanagi, K. Hino, Y. Nagamoto, H. Yoshitake, K. Kishimoto, *Thermoelectric Properties of β-Zn_4Sb_3 Doped with Sn*, *16th International Conference on Thermoelectrics*, IEEE, Piscataway, NJ, 1997, p. 463
45. W. Li, L. Zhou, Y. Li, J. Jiang, G. Xu, *J. Alloys Compd*. **486** (2009) 335
46. P. Kubelka, F. Munk, *Zh. Tekh. Fiz*. **12** (1931) 593
47. P. Kubelka, *J. Opt. Soc. Am*. **38** (1948) 448.